# Thermal Analysis of Greenhouse Gases Using MEMS Based Platinum Microheater

**Shwetha H R**

J. N. N. College of Engineering, Shivamogga, India – 577204.

**Rudraswamy S B**

Sri Jayachamarajendra College of Engineering, Mysuru, India- 570006.

*Abstract* - In semiconductor based chemical sensors, the microheater of a Micro Electromechanical System is crucial. The CleWin 4.1 mask designing tool is used to design a platinum-based microheater, which is then fabricated using the surface micromachining technique. The temperature sensor is integrated with the developed platinum microheater to analyze thermal activity. Using revolutionary research equipment called sensimer, a thermal analysis such as the rising time and fall time of the heater is performed on the $CO_2$ and $CH_4$ selected greenhouse gases. The fabricated microheater with an integrated temperature sensor shows a good response towards the above-mentioned gases and consumes less power. The temperature of the microheater is varied from 30°C to 400°C and then analyzed its performance. From the experimental analysis, we can observe that the power consumed and the average pulsing time constant of the microheater for $CO_2$ gas are 2.8mW and 6ms and for $CH_4$ gas are 3.6mW and 5ms respectively. In this study, the thermal analysis of the above-mentioned greenhouse gas causing materials is described.

*Index Terms* – Greenhouse gases, MEMS, Microheater, Sensimer, Thermal analysis.

## INTRODUCTION

Increased industrialization has undoubtedly helped many countries economic prosperity, but it has also resulted in a significant rise in poisonous gas and other severe environmental pollution emissions. As a result, accurate monitoring of dangerous gases and pollutant detection in the environment has become an inevitable concern in recent years. In this environment, designing robust, low-cost, and portable chemical sensors is required to build a new range of chemical sensors with higher sensitivity. Sensors are devices that convert physical events into data that can be read. Mechanical, electrical, optical, and magnetic types are available.

Various MEMS-based chemical sensors, each operating on distinct criteria such as capacitive, thermal, resistive, and so on, are widely used in the detection of harmful gases. These sensors, which can range in size from a few micrometres to a few centimetres, are produced utilising Integrated Circuit (IC) batch processing processes. On the micro-scale, these sensors can sense, control, and actuate, and on the macro size, they can cause effects. Gas detection sensors are designed to keep the concentrations of certain dangerous gases within a safe limit.

A chemical sensor is made up of a transducer and an active layer that converts chemical data into electrical signals such as frequency, current, and voltage changes. Catalytic sensors, thermal conductivity gas sensors, electrochemical gas sensors, optical gas sensors, infrared gas sensors, semiconductor metal oxide sensors, and acoustic wave gas sensors are some of the gas detecting technologies used to detect harmful gases [1]. Metal Oxide Semiconductors (MOS) are one of these technologies that play a critical role in the detection of target gas concentrations. The development of MEMS chemical sensors based on metal oxide semiconductor technology is the topic of this research. Figure 1 depicts the fundamental structure of a MOS sensor. A MOS sensor is made up of the key layers listed below.

a) Silicon wafer as a substrate
b) Insulating material
c) Microheater
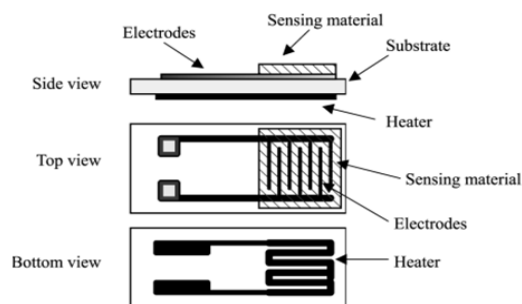d) Interdigitated electrodes and
e) Sensing film



FIGURE 1   : STRUCTURE OF MOS SENSOR

The bottom layer is the substrate, which serves as a foundation for the heater. Silicon is the most used substrate due to its consistent mechanical characteristics. The layer between the substrate and the microheater is known as the insulating platform. An insulating platform is utilised to prevent direct damage to the substrate as well as to limit heat loss. Microheaters are employed in metal oxide gas sensors to properly detect the target gas. The heating of the microheater is done using joules of heat.

Under the sensing layer, integrated electrodes are utilised to determine fluctuations in the resistance of the metal oxide sensor surface as it responds to gases. When the gas is absorbed into the layer, the integration is nothing more than a digit-like pattern of electrodes employed in resistance or capacitance measurement. When the sensor is exposed to air pollutants, the conductivity of the material changes. Integrated chemical sensors are quite popular due to their low cost. Metal oxide sensing layers can be made out of a variety of materials depending on the gas being felt, and they have a high sensitivity to dangerous gases. The conductivity of this layer varies depending on the amount of gas present.

The oxidation or reduction process on the detecting layer of metal oxide sensors occurs at a certain temperature. The number of free electrons on the layer is determined by oxidation or reduction, which increases or decreases the conductivity of the layer. The microheater is crucial in attaining the correct temperature for the reaction. In the design of a microheater, criteria such as homogeneous heating, low power consumption, and mechanical stability must be considered.

When designing microheaters, it is necessary to consider issues such as heat transfer, form, and thermal reaction time, which were not addressed in their work, according to the literature. As previously stated, microheaters transport heat in three ways: conduction, convention, and radiation. For Ti or Pt microheaters, the conduction and convention modes are substantial at temperatures less than 700°C, whereas radiation is minor [2], therefore material selection and temperature sensitivity are critical. The authors used numerical simulation to determine the best material by estimating the greatest temperature and power savings from various insulating layers [3]. Authors devoted similar effort to improving microheater designs in order to obtain power reductions, lower stress profiles, and effective heat distribution [4].

The authors presented tungsten (W) microheaters with thermal response times of up to 2ms at 600°C, focusing on microheater operation. It was discovered to have a power consumption of 12mW [5]. The authors designed a microheater utilising Pt/Ti as a material and achieved a thermal reaction time of 1ms at 400°C with just 9mW of power, despite the fact that they were not tuned for even temperature distribution [6]. The material utilised in MEMS packaging has an impact on total sensing efficiency in practice.

As a result, the author selected packaging materials for a MEMS device that could survive operational circumstances such as high temperature, high pressure, chemical resistance, mechanical and thermal shock, and vibration. Metals, ceramics, silicon, and plastics are the most often utilised materials for micro heater packaging [7]. Metals are good for their robustness, ease of assembly, mechanical integrity, and chemical inertness in severe settings, while ceramics are good for electrically insulating, hermetic sealing, thermal conductivity, chemical inertness, and ease of shape [8].

Microheater packaging, on the other hand, has gotten a lot of attention. When contemplating structural optimization, it's important to remember that the microheater is a small resistance heater that generates heat by delivering an electric current through a filament. The temperature is adjusted via a sophisticated feedback mechanism because the microheater's response time is so short. To control the temperature of the microheater, the authors used Proportional Integral Derivative (PID) controllers [9].

Similarly, feedback control for a microheater in which a conductor's resistance changes with its temperature; hence, the average temperature of a conductor can be calculated by its resistance change [10]. Rather than reading the resistance of the microheater, the temperature of the microheater is commonly determined by the resistance change of an extra metal filament located near the microheater [11]. Different researchers used various types of microheaters. Table 1 displays the findings of a study of different researchers microheaters, as well as the temperature achieved for the amount of electricity, used [12, 13].

As previously stated, substrate materials, filament material, micro-heater material and design, among other things, all have an impact on overall sensitivity or performance. In such cases, determining the best material set and design structures for a MEMS-based gas sensor and flow rate analyzer that will be used for industrial or other purposes is critical. This research focuses on the thermal analysis of greenhouse gases $CO_2$ and $CH_4$ using the Labyrinth, a unique microheater structure that can produce higher temperatures than previous microheater designs for $CO_2$ and $CH_4$ thermal research.

SURVEY ON MICROHEATERS GEOMETRY AND THEIR POWER CONSUMPTION [12,13]

| Design geometry | Average temperature achieved (°c) | Power consumption (mW) |
|---|---|---|
| Double spiral | 375.65 | 2.2 |
| Meander | 330.9 | 2.9 |
| S shape | 380.7 | 3.6 |
| Fan | 372.7 | 2.7 |
| Hilbert order 3 | 376.21 | 3.6 |
| Hilbert order 4 | 360.78 | 3.9 |
| Moore order 3 | 376.66 | 2.5 |
| Moore order 4 | 361.66 | 2.0 |
| Peano order 2 | 379.57 | 3.8 |
| Peano order 3 | 317.38 | 2.9 |

## DESIGN AND FABRICATION OF MICROHEATER

The performance of semiconductor metal oxide gas sensors is determined by the operating temperature of the sensing layer. The operation temperature for various target gases affects the redox processes and response rates on the surface of the sensor film. Because electrical features such as changes in resistance or capacitance of the sensing film require a high temperature to detect, microheaters are a key component in metal oxide semiconductor gas sensors.

Microheaters must have strong heat confinement, high stability, high manufacturing yield, and low power consumption in order to manage temperature distribution along the active region. A suitable microheater shape must be chosen to meet the aforementioned specifications, and the heater's performance can be increased by selecting an optimal high resistive material. Spiral, meander, double meander, and double spiral are the most common microheater structures. The active area temperature remains a hurdle to gas sensor performance, despite the fact that these structures provide average temperature uniformity over the detecting region [14]. We developed, simulated, and analysed three different metals for the proposed MEMS based microheater design to address these challenges, with the goal of improving low power and temperature uniformity.

CleWin 4.1 was used to design the suggested microheater. The heater geometry of a metal oxide semiconductor sensor must be carefully engineered to provide the desired temperature uniformity and overall performance. As a result, the shape of the heating element and the material used to heat it must be carefully determined. Using a high thermal conductivity material, temperature consistency can be attained throughout the heater area [15]. Three different conductive metals, such as Platinum, Titanium, and Tungsten, are used as heating elements with a thickness of 100nm.

To minimise conduction losses, a very thin (20nm) silicon dioxide membrane of size 100µX100µm is used as a high-temperature electrical insulator that supports the heating film [16]. The performance of the heater is directly influenced by the electrical insulators [17]. Good consistency and the required operating temperature disclose the use of heater material. The proposed microheater Labyrinth geometry pattern is shown in Figure 2, and the design geometry dimensions are included in Table 2.
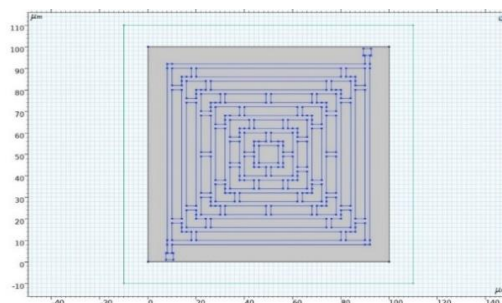


FIGURE 2

LABYRINTH MICROHEATER DESIGN GEOMETRY

TABLE 2

DIMENSIONS OF THE MICROHEATER DESIGN

| Materials used | Pt/Ti/W |
|---|---|
| Area | 100 *100 μm |
| Thickness | 100 nm |
| Width | 2.5 μm |
| Finger gap | 5 μm |

Platinum is a precious metal that has low density, high thermal capacity, and high electrical conductivity, making it one of the rare elements found in the earth's crust. Because of its high melting point, it has good thermal stability, allowing it to tolerate high temperatures and reach the highest temperature for the smallest voltage. Tungsten (W) is a high-temperature, high-mechanical-strength metal [18].

TABLE 3

MATERIAL PROPERTIES FOR PLATINUM

| Parameter | Platinum (Pt) |
|---|---|
| Heat Capacity [J/kg*K] | 133 |
| Young's modulus(E) [Pa] | 168e9 |
| Thermal expansion coefficient($\alpha$) [1/K] | 8.80e-6 |
| Thermal conductivity(k) [W/(m*K)] | 71.6 |
| Density ($\rho v$) [kg/m^3] | 21450 |
| Electric conductivity($\sigma$) [S/m] | 8.9e6 |
| Electric resistivity[$\Omega m$] | 3.4e-7 |

A titanium (Ti) layer is typically used to strengthen the heater's thin film's adherence [19]. Table 3 [20] shows the material properties of microheaters. The microheater is designed by utilising the CleWin 4.1 design tool and surface micromachining process. The developed microheater's schematic geometrical details are illustrated in Figure 3.
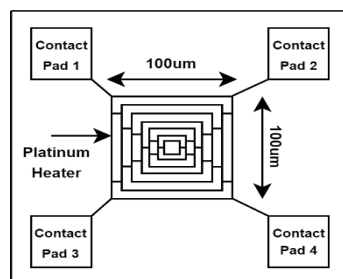


FIGURE 3

SCHEMATIC OF PROPOSED MICROHEATER LABYRINTH DESIGN.

The temperature sensor is built into the planned microheater. As illustrated in Figures 4 (a) & (b), it consists of two suspended platinum coils H and $H^1$ and RTD (temperature sensor) R and $R^1$ (b). The die surface area of the microheater is 2.5mm * 2.5mm, and the membrane size is 100*100μm. The surface micromachining approach was used to create a simulated MEMS microheater structure. RCA1 (Radio Corporation of America standard1) and RCA2 (Radio Corporation of America standard2) protocols are used to clean the silicon substrate. The wafer was incubated in RCA1 solution for 15 minutes at 75°C. RCA1 solution is used to clean the wafer at 75°C for 15 min. The RCA1 and RCA2 cleaning protocol solution ratio is taken as $H_2O$: $NH_4OH$: $H_2O_2$:: 10: 2:2, and $H_2O$: HCl: $H_2O_2$: 12: 2: 2, for HF (Hydrofluoric acid) HF: $H_2O$:: 3: 12: 0 respectively for RCA1 and RCA2 protocols.

After being treated with RCA1 solution, the silicon wafer is rinsed with distilled water before being treated with RCA2 solution to remove any contamination on the wafer surface. The wafer is then placed on a hot plate with a temperature of 270°C to eliminate any remaining fumes. The analytes are then coated thinly on the wafer using the spin coating process. Then, to increase wafer adhesion quality, gentle baking is done by heating the substrate in a furnace to 120ºC for 30 minutes. The substrate is subjected to UV light with a wavelength of 360nm and radiation intensity of 40mJ/cm$^2$ to form pattern pictures.
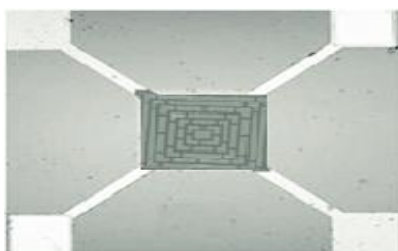
The produced sensor is now developed for 45 seconds using Tetra Methyl Ammonium Hydroxide (TMAH MF26A) and dried with nitrogen gas. The substrate is heated at 100°C for 5 minutes to generate a physical mask that surrounds the wafer and protects it from chemical contamination during etching. To increase the adhesiveness on the wafer surface, the hard baking technique is carried out after soft baking.

The microheater is now subjected to UV photolithography in order to dry etch the photoresist from the wafer. The wafer is then installed on an ICPRIE (Inductively Coupled Plasma Receptive Particle Scratching) equipment to do this. In ICPRIE, an aluminium nitrate base is used to allow for proper warm vitality exchange between the carrier wafer and the MOS substrates. This allows for successful anisotropic etching of the substrate using the Bosch method. Anisotropic carving is done with the gases sulphur hexafluoride ($SF_6$) and octaflurocyclobutane ($C_4F_8$). Table 4 shows the details of the parameters used in ICPRIE anisotropic etching.
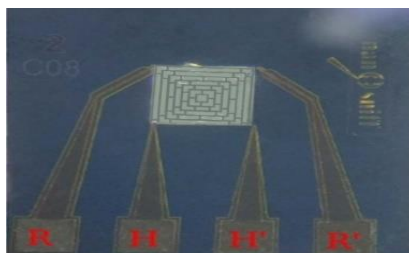
TABLE 4

PARAMETERS USED IN ANISOTROPIC ETCHING

| Variables | Specification |
|---|---|
| Type of Mask | AZ5214 |
| Sulphur hexafluoride ($SF_6$) | 30 SCCM |
| Octaflurocyclobutane ($C_4F_8$) | 70SCCM |
| Inductively Coupled Plasma (ICP) power | 900 W |
| Radio Frequency (RF) Power | 120 W |
| Etch time | 15 sec |
| Chamber pressure | 15 mbar |
| Process temperature | 15°C |

After dry etching, the residue of the photoresist is burned by the ICPRIE instrument. To confirm the removal of unwanted silicon, the optical microscopic inspection was carried out, where the change in colour of the substrate is observed.

(A)

(B)

FIGURE 4

A) MEMS MICROHEATER DESIGN IN CLEWIN SOFTWARE B) SEM IMAGE OF THE DESIGNED MICROHEATER

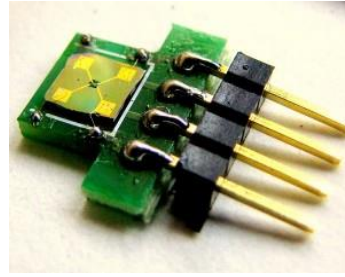The developed sensor as the die after the fabrication is shown in Figure 5.



FIGURE 5

DEVELOPED MICROHEATER DIE SET AFTER FABRICATION WITH FOUR PINS R, R1 H, H1

## EXPERIMENTATION IN SENSIMER

Sensimer microheater tester is used to test the produced microheater. Sensimer is a microheater testing tool that can be used to do thermal analysis on powder or liquid testing materials. As illustrated in Figure 4, the developed microheater comprises four pins. The sensitive electrodes inside the sensimer receive a sinusoidal voltage input, which causes the temperature of the microheater to rise and fall in milliseconds in a pulsating pattern. For all of the investigated materials, the pulse increases and falls times of temperature are measured.

Because each material has a different coefficient of temperature, the rise and fall times of the temperature response are variable for each material. The rise and fall times of temperature vs. time are studied in the experiment for all of the selected greenhouse gases, and the results are provided in the results and discussion section. Figure 6 depicts the device sensimer that was utilised in the study.
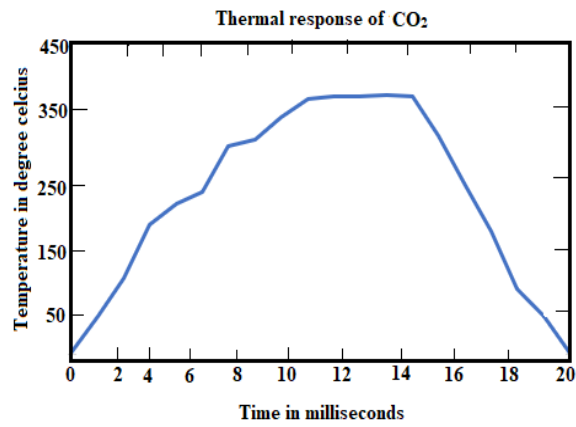


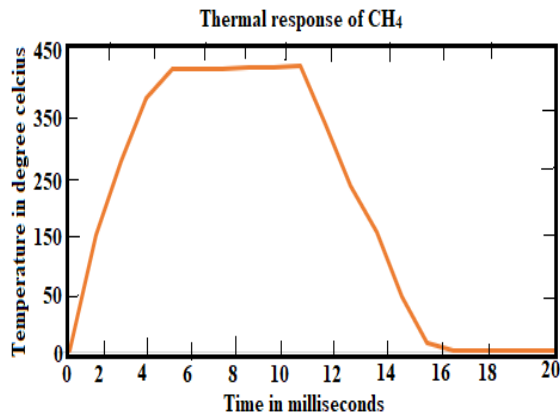FIGURE 6

SENSIMER MICROHEATER TESTING MACHINE

Sensimer is a desktop experimental device that allows you to change the temperature of a microheater in order to study its thermal response. It is made out of a microheater plug-in port and related electronics, as well as software to control electrical excitation. The graph of temperature vs. time depicts the thermal mass response of a microheater for a material.

## RESULTS AND DISCUSSIONS

At the end of the paper, you must include a list of references. If it's not absolutely essential, start them on a new page. Every reference in the text should also appear in the list of references, and vice versa. In the text, use [1] or [2], [3] to indicate references. In this study, the selected greenhouse gases $CO_2$ and $CH_4$ are tested in powder form in a microheater. The thermal responses of $CO_2$ and $CH_4$ are evaluated independently, and then the rise and fall times of both thermal mass are compared, in order to study the temperature sensitivity of selected greenhouse gases. Figure 7 depicts the thermal reaction of greenhouse gases.

## Thermal response of $CO_2$



(A)

## Thermal response of $CH_4$



(B)

FIGURE 7

Thermal response greenhouse gases (A) $CO_2$ (B) $CH_4$

The rising period of $CO_2$ is 10ms, and the fall time is 6ms, according to the graph in Figure 7 (a). We may deduce from the graph in Figure 7 (b) that the rising time of $CH_4$ is 5ms and the fall time is 6ms.
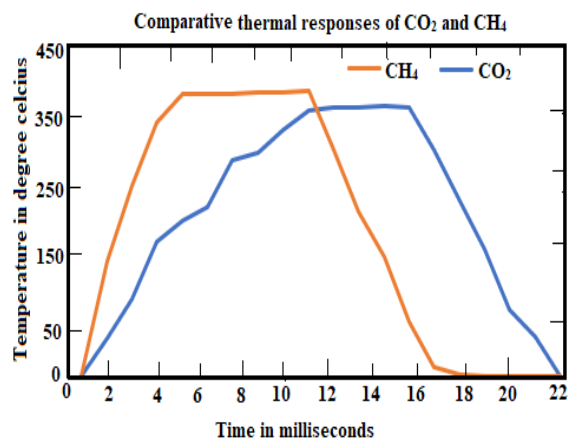
## Comparative thermal responses of $CO_2$ and $CH_4$



FIGURE 8

COMPARISON OF THERMAL RESPONSES OF $CO_2$ AND $CH_4$

Figure 8 shows a comparison graph of $CO_2$ and $CH_4$ temperature responses, which is summarised in Table 5. Carbon dioxide ($CO_2$) molecules have a unique property that allows them to absorb energy from infrared (IR) light. The $CO_2$ molecule vibrates as a result of the photon's energy. The molecule subsequently gives up this extra energy by emitting another infrared photon later. Once the extra energy is removed by the emitted photon, the carbon dioxide molecule stops vibrating [21].

$CO_2$ molecules are often flowing, striking with other gas molecules and transferring energy from one molecule to the next. A $CO_2$ molecule will most certainly collide with multiple other gas molecules before re-emitting the infrared photon in the more complex real-world process. The energy gained from the absorbed photon could be transferred by the $CO_2$ molecule to another molecule, increasing the speed of that molecule's motion. Because the temperature of a gas is proportional to the speed of its molecules, the quicker motion of a molecule caused by an IR photon absorbed by a $CO_2$ molecule boosts the temperature of the gas [22].

$CO_2$ requires a high-temperature environment to be detected due to its enhanced heat-absorbing capacity. As a result, a microheater with a temperature of 390°C was designed to shatter the $CO_2$ atoms on the sensor, as shown in Figure 7. (a). When compared to oxygen and nitrogen, which can break at 60–70°C [23], this is a pretty high temperature. The ability to absorb more heat increases as the gas concentration rises.

Methane, which comprises one carbon atom and four hydrogen atoms, is a more potent gas in the atmosphere than $CO_2$. It contributes more to the greenhouse problem while being present in much fewer quantities than $CO_2$ [24]. In comparison to $CO_2$, methane has a very high IR radiation absorption capability, which allows it to store more heat [25]. As a result, breaking the atoms of $CH_4$ required more heat from the microheater than breaking the atoms of $CO_2$, as illustrated in Figure 7. (b). The $CH_4$ microheater heat was 419°C, while the $CO_2$ microheater heat was 390°C. A comparison graph of both $CO_2$ and $CH_4$ is presented in Figure 8.



FIGURE 9

IMAGES OF THE PROPOSED LABYRINTH MICROHEATER STRUCTURE WITH AND WITHOUT APPLICATION OF SINUSOIDAL VOLTAGE.

Table 5 will provide a summary of the findings. We may deduce that the power consumption of the microheater to reach the maximum temperature for $CH_4$ is higher than for $CO_2$. The power is calculated by multiplying the supply voltage and constant current of the sensimer machine.

The proposed labyrinth microheater structure is explained using a sensimer device. The microheater produces pulsating output when fed a sinusoidal voltage, and when the temperature is elevated to a very high level, the microheater appears red hot. The voltage supply to the microheater before and after it was applied is shown in Figure 9.

TABLE 5

CHARACTERISTICS OF LABYRINTH MICROHEATER

| Sl. No. | Material | Voltage Applied | Raise Time | Fall Time | Power Consumed | Average Temperature Achieved |
|---|---|---|---|---|---|---|
| 1. | $CO_2$ | 3.5mV | 10ms | 6ms | 2.8mW | 390°C |
| 2. | $CH_4$ | 4.5mV | 5ms | 6ms | 3.6mW | 410°C |

## CONCLUSION

The design and thermal analysis of a platinum-based new Labyrinth microheater for $CO_2$ and $CH_4$ greenhouse gases were the subjects of this study. We used the CleWin 4.1 design tool to design the proposed microheater geometry and a unique sensimer device is used for thermal analysis. The experimental results show that the proposed Labyrinth microheater structure can achieve the highest temperature with the least amount of power than other traditional microheater structures. We found that a proposed microheater used to break $CO_2$ atoms had an average temperature of 390°C, whereas a microheater used to break $CH_4$ atoms had an average temperature of 419°C. We may infer that when we vary the heater temperature from 30°C to 400°C the power consumption and average pulsing time constant for $CO_2$ and $CH_4$ gases are 2.8mW and 6ms and 3.6mW and 5ms, respectively.

**REFERENCES**

[1] Spruit, Ronald and Omme, J et. al. (2017) "A Review on Development and Optimization of Microheaters for High-Temperature in Situ Studies," *Journal of Microelectromechanical Systems*,1-18.

[2] Creemer, J.F., Briand, D. and Zandbergen, Henny et. al. (2008) Microhotplates with TiN heaters. *Sensors and Actuators A: Physical.* 148. 416-421.

[3] Adrian P, and Mouritz, (2012 ) "Introduction to Aerospace Materials," *Materials selection for aerospace* Editor(s): Woodhead Publishing, 569-600.

[4] Khalid, M., Abu Bakar, Mohamad, et. al. (2011) "Effect of heater geometry on the high temperature distribution on a MEMS micro-hotplate," *Proceedings of the 3rd Asia Symposium on Quality Electronic Design, ASQED* 2011.

[5] Jeroish, Z.E., Bhuvaneshwari, K.S., Samsuri, F. et al. (2022) "Microheater: material, design, fabrication, temperature control, and applications—a role in COVID-19," *Biomed Microdevices* 24**,** 3.

[6] Ali, Syed Zeeshan, Udrea, Florin, Milne, W., et al. (2009) "Tungsten-Based SOI Microhotplates for Smart Gas Sensors," *Microelectromechanical Systems,* 17, 1408 - 1417.

[7] Raj S. Amiri, M.M. Ariannejad, D. Vigneswaran, C.S. Lim, P. Yupapin, (2018) "Performances and procedures modules in micro electromechanical system packaging technologies," *Results in Physics*,11, 306-314.

[8] Prasad, K., Bazaka, O., Chua, M., Rochford, M., Fedrick, L., et. al. (2017) "Metallic Biomaterials: Current Challenges and Opportunities," *Materials (Basel, Switzerland)*, *10*(8), 884.

[9] Harles Manière, Geuntak Lee, Eugene A. Olevsky, (2017) "Proportional integral derivative, modeling and ways of stabilization for the spark plasma sintering process," *Results in Physics*,7,1494-1497.

[10] Darrin, Ann and Osiander, Robert. (2011) "MEMS Packaging Materials," *MEMS Materials and Processes Handbook*," 879-923.

[11] Guan, Teck and Puers, Robert (2010) "Thermal Analysis of a Ag/Ti Based Microheater," *Procedia Engineering*, 5, 1356-1359.

[12] Vasiliev, Alexey, Nisan, Anton, Samotaev, Nikolay (2017) "Aerosol/ink Jet Printing Technology for High-Temperature," *MEMS Sensors. Proceedings*, 1, 617.

[13] Toskov, Sasa, & Glatz, Ronald & Miskovic, Goran & Radosavljevic, Goran. (2013) "Modeling and fabrication of Pt micro-heaters built on alumina Substrate," *Proceedings of the International Spring Seminar on Electronics Technology*, 47-52.

[14] Kahroba, P. Mirzaee, I. Sharifi, P. Shirvani, H. (2008) "The microcavity-based micro-heater: an optimum design for micro-heaters," *Microsystem Technologies*, 14, 705–710.

[15] Moon, J.M.B.U. Lee, C.H. Shim, M.B. Lee et. al. (2005) "Silicon bridge grill micro-gas sensor array," *Sensors and Actuators B: Chemical*, 108, 271–277.

[16] Abdennaceur Kachouri, Hekmet Samet (2014) "Design and electro-thermal analysis of a platinum micro heater for gas sensors," *Journal of Engineering and Applied Sciences*, 9, 2307–23014.

[17] Saxena, G., Paily, R. (2015) "Performance improvement of square microhotplate with insulation layer and heater geometry," *Microsystem Technologies*, 21.

[18] Kumar, N. and Mehta, N. (2013) "Applications of Different Numerical Methods in Heat Transfer-A Review," *International Journal of Engineering Sciences & Research Technology*, 4, 7–7.

[19] Ali, Z.S., Udrea, F., Milne, W.I., Gardner, J.W. (2008) "Tungsten-Based SOI Microhotplates for Smart Gas Sensors," Journal of *Microelec- tromechanical Systems*, pp. 17–17.

[20] Sureshkannan, G. and Kumar, G.M. (2012) "Experimental Investigation and 2- D Thermal Analysis of High Temperature Microtubular Heater," *European Journal of Scientific Research*, 74, 403–411.

[21] Aldoshin, G. and Yakovlev, S. (2015) "Analytic model of vibrations of a carbon dioxide molecule Fermi resonance," *Mechanics of Solids*, 50, 33-43.

[22] Thomas R. Anderson, Ed Hawkins, Philip D. Jones, (2016) "CO2, the greenhouse effect and global warming," *the pioneering work of Arrhenius and Callendar to today's Earth System Models, Endeavour*,40,3,178-187.

[23] Kim, J., Ha, H., Doh, W.H. et al. (2020) "How Rh surface breaks $CO_2$ molecules under ambient pressure," *Nat Commun* 11, 5649.

[24] Darkwah, Williams Kweku, Odum, Bismark, Addae, et. al. (2018) "Greenhouse Effect: Greenhouse Gases and Their Impact on Global Warming" *Journal of Scientific Research and Reports*. 17. 1-9.

[25] Hdr, Zdgvbdh & Tan, Qiulin & Wendong, Zhang & Chenyang, Xue & Tao, Guo & Jijun, Xiong. (2011) "Miniature low-power IR monitor for methane detection," *Measurement*. 44. 823-831.